



HAL
open science

Using a dose-area product for absolute measurements in small fields: a feasibility study

Stéphane Dufreneix, Aimé Ostrowsky, Maiwenn Le Roy, Line Sommier, Jean Gouriou, Franck Delaunay, Benjamin Rapp, Josiane Daures, jean-marc bordy

► To cite this version:

Stéphane Dufreneix, Aimé Ostrowsky, Maiwenn Le Roy, Line Sommier, Jean Gouriou, et al.. Using a dose-area product for absolute measurements in small fields: a feasibility study. *Physics in Medicine and Biology*, 2016, 61 (2), pp.650 - 662. 10.1088/0031-9155/61/2/650 . hal-01864082

HAL Id: hal-01864082

<https://hal.science/hal-01864082>

Submitted on 3 Oct 2023

HAL is a multi-disciplinary open access archive for the deposit and dissemination of scientific research documents, whether they are published or not. The documents may come from teaching and research institutions in France or abroad, or from public or private research centers.

L'archive ouverte pluridisciplinaire **HAL**, est destinée au dépôt et à la diffusion de documents scientifiques de niveau recherche, publiés ou non, émanant des établissements d'enseignement et de recherche français ou étrangers, des laboratoires publics ou privés.

Using a dose-area product for absolute measurements in small fields: a feasibility study

S Dufreneix, A Ostrowsky, M Le Roy, L Sommier, J Gouriou, F Delaunay, B Rapp, J Daures, and J-M Bordy*

CEA, LIST, Laboratoire National Henri Becquerel (LNE-LNHB), F-91191 Gif-sur-Yvette, France

*E-mail: jean-marc.bordy@cea.fr

Abstract. To extend the dosimetric reference system to field sizes smaller than 2 cm x 2 cm, the LNE-LNHB laboratory is studying an approach based on a new dosimetric quantity named the dose-area product instead of the commonly used absorbed dose at a point. A graphite calorimeter and a plane parallel ion chamber with a sensitive surface of 3 cm diameter were designed and built for measurements in fields of 2, 1 and 0.75 cm diameter. The detector surface being larger than the beam section, most of the issues linked with absolute dose measurements at a point could be avoided. With Monte Carlo simulations, calibration factors of the plane parallel ionization chamber could be established in terms of dose-area product in water for small fields with an uncertainty smaller than 0.9 %.

1. Introduction

Absorbed dose measurement in small field is a challenging area (IPEM, 2010): because of lateral electronic disequilibrium, partial source occlusion, detector size and its non-water equivalence, the absolute and relative dose determination is associated to significant uncertainty (Das et al., 2008).

In order to develop standardized recommendations for dosimetry procedures and detectors (Alfonso et al., 2008) suggested a new formalism for reference dosimetry of small and non-standard fields. It introduced a new correction factor $k_{Q_{msr},Q}^{f_{msr},f_{ref}}$ which depends on the detector and the delivery machine. Numerous studies have determined this correction factor by Monte Carlo simulations or by measurements (Benmakhlouf et al., 2014, Moignier et al., 2014), allowing traceable dosimetry for small fields in radiotherapy departments.

An alternative way to establish reference dosimetry in small fields is to develop appropriate primary standards and dosimetric protocols in National Measurements Institutes. However, no primary standards are currently available in small fields. Recently, the French and German primary laboratories LNE-LNHB and PTB showed that the calibration factor of cylindrical ionization chambers was rather independent of field size for square fields which sizes are between 10 and 2 cm (Le Roy, 2011, Delaunay

et al., 2012, Krauss and Kapsch, 2014). The French dosimetric standards in the 4 cm x 4 cm and 2 cm x 2 cm fields were established with a small graphite calorimeter (Daures et al., 2012). Measurements could be considered punctual by applying a correction factor which took into account the inhomogeneity of the dose deposition over the 0.6 cm diameter sensitive surface. The miniaturization limit of primary dosimeters was reached during this study.

Consequently, the notion of absorbed dose to water at a point can no longer be used for absolute measurements in a primary laboratory for fields smaller than 2 cm x 2 cm. This field size can be considered as small since dosimetric measurements are usually disturbed by the lack of lateral electronic equilibrium, spectral changes and partial occlusion of the source under 3 cm x 3 cm (Das et al., 2008). (Alfonso et al., 2008) also suggest that a small field is defined as a field with a size smaller than the lateral range of charged particles. The minimal radius needed to achieve complete lateral electronic equilibrium being of 1.3 g.cm⁻² at 6 MV (Li et al., 1995), a 2 cm x 2 cm can be considered as small at 6 MV.

A new approach has been suggested in order to bring the calibration conditions closer to the clinical use (figure 1) (Ostrowsky et al., 2010): by using detectors larger than the beam, difficulties specific to measurements in small fields like the selection of a small and good detector as well as misalignments issues are overcome. This idea was already investigated for output factor measurements (Djouguela et al., 2006, Fan et al., 2009, Sanchez-Doblado et al., 2007, Underwood et al., 2013) but never for primary measurements with the view to establish dosimetric standards in small fields.

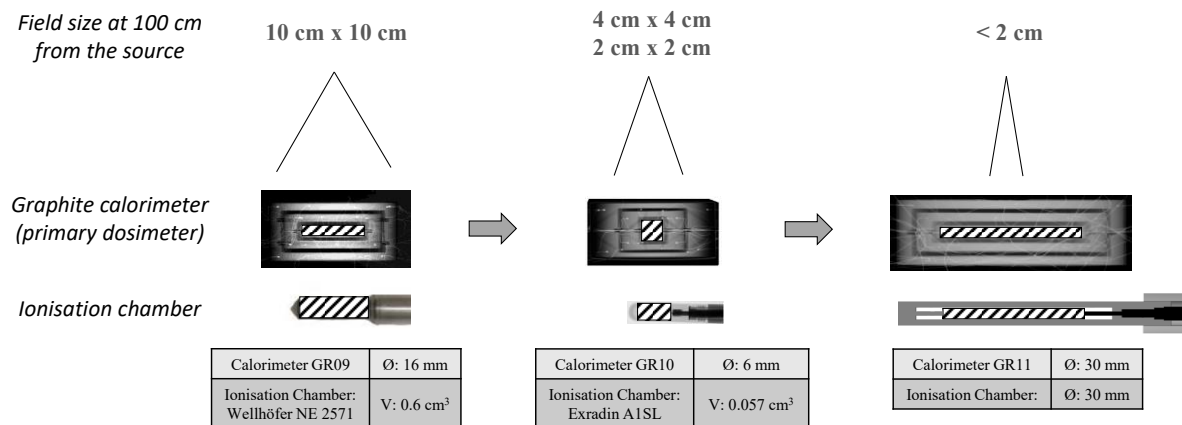


Figure 1: From left to right: chronological evolution of the establishment of dosimetric references in broad and small fields at LNE-LNHB (sensitive volumes are hatched).

This paper presents the feasible study realised at the LNE-LNHB laboratory on the use of the dose-area product in small fields of 2, 1 and 0.75 cm diameters using a graphite calorimeter and a plane-parallel ionization chamber with a large sensitive surface. The Monte Carlo simulations needed for the graphite / water correction factor are described and the calibration factors of the large ionization chamber are presented. Unless otherwise stated, all uncertainties are given for $k = 1$. In agreement with the Guide to the Expression of Uncertainty in Measurement (JCGM, 2008), the number in parentheses after a value

is the numerical value of the combined standard uncertainty referred to the corresponding last digits of the quoted result.

2. Theory

Since the sensitive volumes of large detectors used for measurements in small fields are no longer homogeneously irradiated, a new dosimetric quantity has to be introduced for dosimetry in small fields: the dose-area product (DAP). It represents the energy deposited by the beam over the sensitive surface of the detector and is expressed in Gy.cm². Due to the technical specification of the calorimeter and the plane parallel chamber built for this study, all dose-area products described in this paper will be defined for a sensitive surface of 3 cm diameter.

By definition, the variation of the dose-area product with the off-axis distance depends of the absorbed dose deposited and the off-axis distance. If a radial symmetry of the dose distribution can be assumed, the contribution of the absorbed dose D_{abs} deposited by the irradiation beam at distance r from the axis is $\pi r^2 D_{abs}$. As a consequence, even if the highest dose is deposited on the axis, its contribution to the dose-area product is null ($r = 0$). On the contrary, out-of-field doses cannot be neglected. The highest contribution of an irradiation beam to a dose-area product is in the penumbra region where the absorbed dose and the off-axis distance are both important.

The dose-area product is already widely used in radiology to express the total x-ray flux in the beam. It was shown invariant in air with distance from the focal spot (ICRU 74, 2005). The main difference with the dosimetric quantity suggested above for radiotherapy is the surface considered: surface of the beam in radiology and surface of the dosimeter in radiotherapy. The medium considered is also different, modifying the scattering out of the beam.

The calibration factor of a large ionization chamber (which has the same sensitive surface as the graphite calorimeter used for primary measurements) in terms of dose-area product N_{DAPw} can be defined as:

$$N_{DAPw} = \frac{DAP_{w/MU}(S)}{Q_{w/MU}^*} = \frac{D_{core/MU}}{Q_{w/MU}^*} \left[\frac{D_w(V)}{D_{core}} \right]_{MC} S$$

where:

- $DAP_{w/MU}(S)$ is the dose-area product in water over a sensitive surface S per monitor unit;
- $Q_{w/MU}^*$ is the charge collected by the large ionization chamber per monitor unit corrected from leakage current, temperature, pressure, polarity and recombination;
- $D_{core/MU}$ is the absorbed dose measured by the large calorimeter per monitor unit;
- $\left[\frac{D_w(V)}{D_{core}} \right]_{MC}$ is the graphite / water correction factor determined by Monte Carlo simulation

If the calibration factor of a large ionization chamber is independent of field size, output factors in terms of dose-area product would be equal to the ratio of the ionization chamber readings, without applying any correction factor.

3. Materials and methods

3.1. Linear accelerator

All measurements were realised in a 6 MV beam, which is an energy commonly used with small fields in IMRT, arctherapy, stereotactic radiotherapy and radiosurgery. The Saturn 43 (General Electrics) of the laboratory was used. Small circular fields were delimited by an additional collimator made of tungsten, 10 cm thick and localized after the collimation system of the irradiation head. Two monitor chambers were located between the irradiation head and the additional collimator to measure beam fluctuations during irradiation. A dedicated support allowing rotations around the three axes allowed for a precise alignment of the collimator on the beam axis. Profiles measured at 10 cm depth in water confirmed that the beam shapes were not elliptical but circular.

3.2. Graphite calorimeter

A new graphite calorimeter was specially built at the LNE-LNHB for this study. Its construction was largely inspired from previous calorimeters (Daures and Ostrowsky, 2005) but its dimensions were larger than usual (figure 1): the sensitive volume (named the core) is a graphite cylinder of 3 cm diameter and 0.3 cm height, surrounded by a jacket and a shield which are thermally regulated. These three elements are separated by vacuum gaps. Heating and measurements were realised with BR14 thermistors (General Electrics Sensing) which resistance varies with temperature. The final radiograph of the calorimeter as seen by the beam is shown in figure 2.

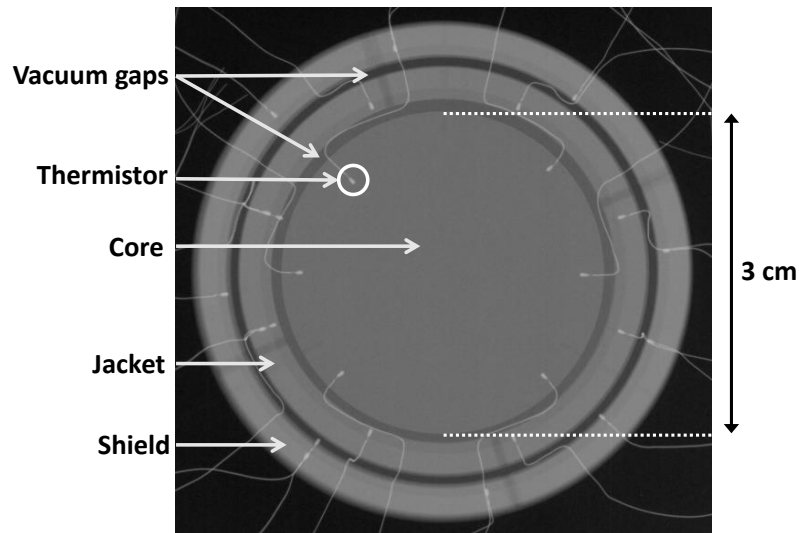


Figure 2: Radiograph of the large graphite calorimeter.

The calorimeter was always used in a quasi-adiabatic mode: the core and jacket temperatures rise under irradiation while the shield temperature is kept constant. The temperature of the jacket is regulated by means of a numerical PID (proportional–integral–derivative) controller to follow the core temperature. One thermistor in the core and one in the jacket constitute two arms of a Wheatstone bridge. The regulating electrical power is calculated from the bridge disequilibrium and dissipated in the jacket

Towards the use of a dose-area product for absolute measurements in small fields

through six thermistors. As the temperatures of the core and jacket are close together, the thermal transfers are minimized.

Before the measurement, a calibration by electrical substitution has to be performed under the same thermal conditions. The expression of the electrical calibration coefficient C'_p is:

$$C'_p = \frac{Q_{el}}{m \cdot \Delta T'_{el}}$$

where $\Delta T'_{el}$ is the variation of the temperature in the core during electrical heating measured with a thermistor associated with a very precise Wheatstone bridge, Q_{el} is the heat quantity dissipated in the core by the Joule effect through heating thermistors and m is the mass of the core.

Thereafter the mean absorbed dose in the core \bar{D} is given by:

$$\bar{D} = C'_p \Delta T' k_i$$

where $\Delta T'$ is the variation of the temperature in the core during irradiation. k_i is the corrective factors for the impurities in the core if the absorbed dose to the graphite was given in a homogeneous graphite material.

The quasi-adiabatic mode requires a precise determination of the mass of the core. Measurements realized during the assembly and summarized in table 1 led to an uncertainty of 0.009 %.

	Mass (mg)	%
Graphite	3773.968 (05)	99.65
Thermistor (+ wires)	6.648 (30)	0.18
Kapton tubes	0.595 (05)	0.01
Glue	6.050 (09)	0.16
Core	3787.26 (32)	100.00

Table 1: Mass of the different components of the calorimeter's core.

This large calorimeter was tested and compared to previously built graphite calorimeters in a ^{60}Co beam under reference conditions: the point of measurement is considered at the middle of the core and placed at 100 cm from the source and 5 g.cm⁻² depth in a 10 cm x 10 cm beam. The absorbed dose rate in water could be determined with an uncertainty of 0.34 % and was found in good agreement with the results of two other calorimeters previously studied (Daures et al., 2012) (figure 3).

Towards the use of a dose-area product for absolute measurements in small fields

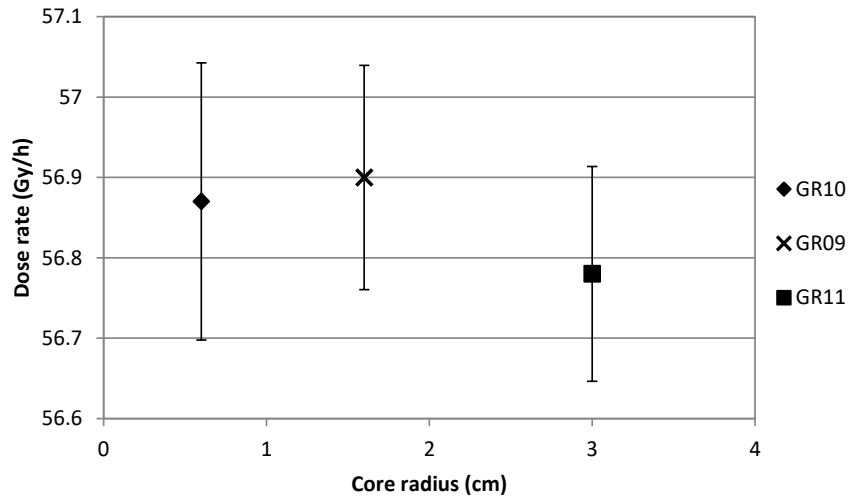


Figure 3: Dose rates measured in a 10 cm x 10cm ^{60}Co beam with different calorimeters.

For a better statistic in small fields, between 85 and 185 calorimetric measurements were realised for each field size, all corrected from the monitor response. An electric calibration of the calorimeter was realised every 6 measurements in order to link the rise in temperature that occurs in the core under irradiation to the absorbed dose value. Since the sensitive surface of the calorimeter is larger than the beam section, the temperature rise induced under irradiation in the core decreases with field section: for 5 min irradiations in a 6 MV beam, the temperature rise is of 4 mK in the 2 cm diameter field, 1 mK in the 1 cm diameter field and 0.6 mK in the 0.75 cm diameter field. As shown on figure 4, the large calorimeter can measure such small temperature rises even though thermic fluctuations measured during background are of approximately 30 μK . All calorimetric measurements in small fields were conducted in a 30 cm x 30 cm x 20 cm graphite phantom with the middle of the core located at 100 cm from the source and 10 $\text{g}\cdot\text{cm}^{-2}$ depth.

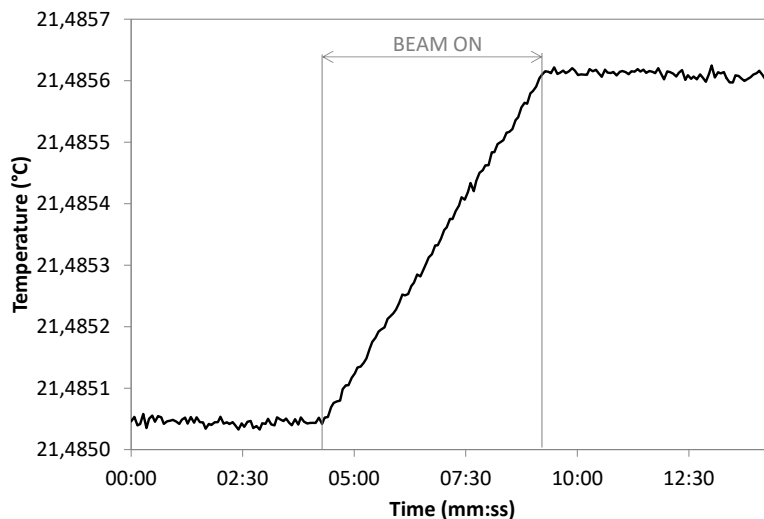


Figure 4: temperature rise in the core of the large calorimeter in a 0.75 cm diameter beam.

3.3. Large plane parallel ionization chamber

A single volume plane parallel ionization chamber was also designed and built at the laboratory for calibration in terms of dose-area product. Its sensitive surface is a cylinder of 3 cm diameter and 0.2 cm height so that the beam is integrated over the same sensitive surface with the ionization chamber and the graphite calorimeter. The sealing box was made out of PMMA but this material was found to deform in water, causing a shift of around -0.6 % per hour on the chamber response: the deformation was applying a constraint on the electrodes, varying the thickness of the detection volume. Measurements in a ^{60}Co beam over several months were within 0.2 % showing that this shift in water was reversible and could thus be corrected. With a nominal voltage of 200 V (i.e. 100 V / mm), the leakage current was smaller than 10^{-15} A and reproducibility was equal to 0.14 %.

Like for all ionization chambers, a recombination factor k_s had to be applied. However, the usual formula described in the TRS 398 (IAEA-TRS398, 2006) could not be applied since the chamber is partially irradiated in small fields. Recombination effects were assumed spatially invariant. The recombination correction factor was determined using the asymptote of $1/Q$ against $1/V$ around the nominal voltage of 200 V measured at 100 cm from the source for a pulse frequency of 200 Hz and a dose per pulse of 0.13 mGy at 10 cm depth (figure 5). Results at 10 and 20 cm depth are given in table 2; a global relative uncertainty of 0.05 % was achieved.

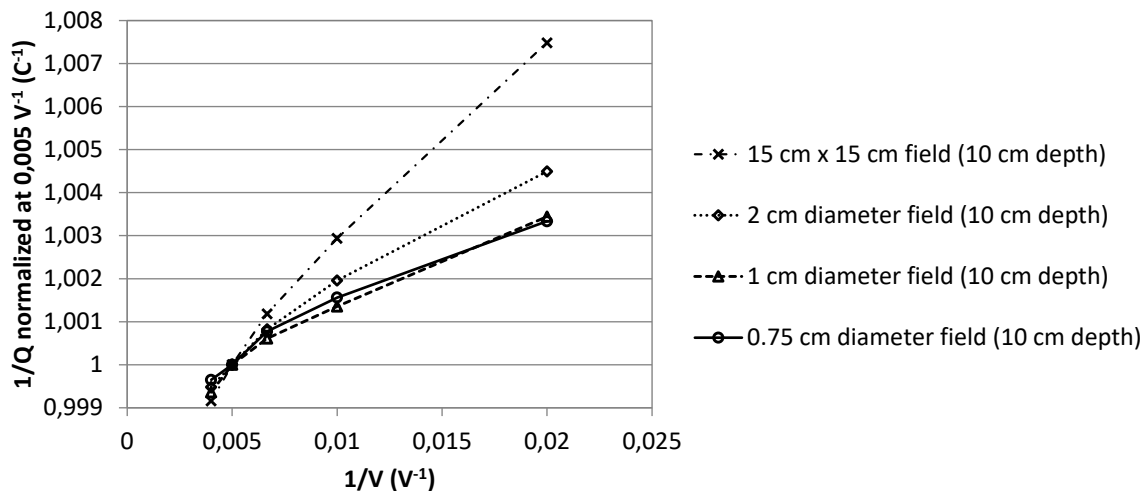


Figure 5: Jaffé plots for the large plane parallel ionization chamber in different irradiation fields. For better clarity, only measurements at 10 cm depth are represented.

Beam size	Depth (cm)	k_s
15 cm x 15 cm	10	1.0038
2 cm diameter	10	1.0025
	20	1.0025
1 cm diameter	10	1.0024
	20	1.0021
0.75 cm diameter	10	1.0021
	20	1.0016

Table 2: Recombination factors for the large plane parallel ionization chamber.

For the polarity correction factor, the usual formula of TRS398 was used.

A 2 mm misalignment of the large ionization chamber in a 2 cm diameter field lead to a 0.5 % under-response (0.3 % in a 1 cm and 0.75 cm diameter field). A precise alignment of the large chamber on the beam axis is thus not as critical as when a punctal dose has to be measured with a small detector.

3.4. Monte Carlo simulations

Two codes were used in this study: EGSnrc version 4.22.4 (Kawrakow, 2000, Kawrakow et al., 2009) and a parallel version of PENELOPE 2006 (Salvat et al., 2006). Each code was used by a different user to prevent from systematic errors. The Saturne 43 head was modelled and the initial parameters of the electrons were determined: mean energy, spectral dispersion and spatial dispersion.

Adjustment of the parameters were realised by comparing the lateral and depth dose variations simulated to measurements. For the 2 cm diameter field, dose profiles were measured with a PinPoint PTW_31014 ionization chamber which sensitive volume has a 2 mm diameter and EBT3 films scanned with a 360 dpi. For the 1 and 0.75 cm diameter fields, only profiles measured with EBT3 were used for comparison. Depth dose variations were measured with a small ionization chamber: an Exradin A1SL in the 2 cm diameter field and a PTW_31014 in the 1 and 0.75 cm diameter fields. The Exradin A1SL was not used for the two smallest diameter beams because its sensitive volume has a 4 mm diameter which is too large for small field measurements. Depth dose variations were also measured with the large ionization chamber previously described because it is less sensitive to a drift of the chamber center from the beam axis when depth increases. For the simulation of lateral and depth dose variation, the voxel size was adjusted to the sensitive volume of the detector used during measurements so that the averaging effect could be taken into account and a direct comparison could be performed. All modelled distributions passed a global gamma analysis with a 0.5 % / 1 mm criteria.

4. Results and discussion

4.1. Small fields characteristics

In order to quantify the attenuation of the beam, the $DAPR_{20,10}$ was defined as the ratio of the dose-area product measured at 20 and 10 g.cm⁻² depth with the large ionization chamber, corrected from recombination. The source-detector distance was kept constant at 100 cm. As shown in table 3, the variation of the $DAPR_{20,10}$ with field size is small.

Beam diameter (cm)	$DAPR_{20,10}$
2	0.6435 (10)
1	0.6444 (9)
0.75	0.6445 (8)

Table 3: $DAPR_{20,10}$ of the three small fields studied at 6 MV.

Relative dose variation with depth was measured using the large ionization chamber and a PinPoint PTW_31014 chamber. The measurement depth was varied with a fixed SSD at 90 cm. The PinPoint measurements are sensitive to the attenuation and scattering of the beam by the medium but

Towards the use of a dose-area product for absolute measurements in small fields

also to the decrease of the photon fluence on the beam axis due to the increasing of the distance from the source. Correcting mathematically for the inverse square law, the PinPoint measurements are in good agreement with the large ionization chamber measurements (figure 6). This shows that all photons coming from the source are collected by the sensitive surface of the large ionization chamber at any depth and that this chamber is only measuring the attenuation and scattering of the beam.

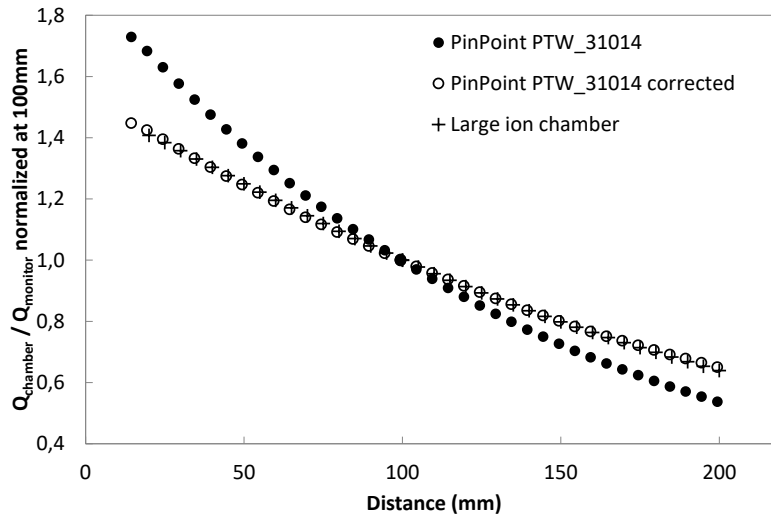


Figure 6: Relative dose variations in a 1 cm diameter beam measured with a large ionization chamber and a PinPoint at 6 MV.

4.2. Graphite / water correction factors

A graphite / water correction factor was determined to convert the absolute measurement in graphite obtained by calorimetry to a mean absorbed dose in water. The absorbed energy was recorded in the core of the simulated calorimeter and in a water volume with the same dimensions than the core (cylinder of 3 cm diameter and 0.3 cm height) surrounded by water. Cut-off energies were set to 5 keV for photons and 50 keV (PENELOPE) or 10 keV (EGSnrc) for charged particles.

Graphite / water correction factors are given in table 4 (only statistical uncertainties are given). By applying a type B uncertainty of 0.4 % for each code, all correction factors are in agreement. Considering that each code was used independently, these results are very satisfying. For the rest of this study, the mean of the PENELOPE and EGSnrc values were used.

Beam diameter (cm)	PENELOPE	EGSnrc	PENELOPE / EGSnrc
2	1.0085 (10)	1.0062 (08)	1.0023 (13)
1	1.0082 (19)	1.0079 (05)	1.0003 (19)
0.75	1.0089 (30)	1.0088 (08)	1.0000 (31)

Table 4: Graphite / water correction factors simulated with PENELOPE and EGSnrc. Only statistical uncertainties are given.

The comparison of graphite / water correction factors determined by Monte Carlo to measurement is difficult: Fricke measurements in a graphite and a water phantom were conducted in the 2 cm diameter field using a 3 cm diameter flask but uncertainties on the measurements were too large for a precise validation of the factors determined by Monte Carlo.

It was thus decided to compare the ratio of the absorbed doses measured and simulated in the core of a small calorimeter (named GR10; $\varnothing=0.6$ cm; see figure 1) and in the core of a large calorimeter (named GR11; $\varnothing=3$ cm). Because of the size of the small calorimeter GR10, calorimetric measurements could only be conducted in the 2 cm diameter field. Experimental and calculated results given in table 5 show a large difference between simulations and measurements, outside the uncertainties. Results obtained with the two Monte Carlo codes are also in disagreement. Because this difference between simulations and measurements was unexpected, calculations were conducted a second time with smaller cut-off energies. For PENELOPE, the following parameters were selected: $E_{\text{abs}}(\text{photons}) = 1$ keV, $E_{\text{abs}}(\text{electrons}) = E_{\text{abs}}(\text{positons}) = 10$ keV, $C_1 = C_2 = 0.05$. For EGSnrc, the following parameters were selected: $\text{PCUT} = \text{AP} = \text{AE} = 1$ keV, $\text{ECUT} = 512$ keV, $\text{ESTEPE} = 0.1$ and $\text{XIMAX} = 0.1$. Results differ from previous values of 0.04 % (PENELOPE) and 0.06 % (EGSnrc).

	$D_{\text{core}}(\text{GR10}) / D_{\text{core}}(\text{GR11})$	$D_{\text{core}}(\text{GR10}) / D_{\text{core}}(\text{GR11})$ compared to measurements
Measurements	2.1936 (59)	1
PENELOPE	2.2127 (58)	1.0087 (38)
EGSnrc	2.2243 (45)	1.0140 (34)

Table 5: Comparison of the dose ratio GR10 / GR11 determined from calorimetric measurements and from simulations in the 2 cm diameter beam.

The difference observed between simulations and measurements could be due to the fact that for the small calorimeter, the voxel simulating the core is fully irradiated whereas for the large calorimeter the voxel simulating the core is only partially irradiated. If the energy deposited by low energy photons is not precisely taken into account, the scattered beam in the penumbra and out of field regions could be incorrectly simulated, introducing a bias. Interesting to note is that a good agreement is found between the two Monte Carlo codes when the dose absorbed in two voxels with the same dimensions and larger than the beam is compared (as in table 4). The uncertainty on the graphite / water correction factors mentioned in table 4 could however be larger than indicated.

4.3. Calibration factors

All data and correction factors needed to determine the calibration factors are summarized in table 6. One can notice the low uncertainty that can be achieved on dosimetric references in small fields using a dose-area product.

	2 cm diameter beam		1 cm diameter beam		0.75 cm diameter beam	
$\frac{D_{\text{core}}/\text{MU}}{Q_{\text{w}}/\text{MU}} (x10^7 \text{ Gy.C}^{-1})$	2.2177	0.59 %	2.1765	0.32 %	2.1766	0.61 %
$\left[\frac{D_{\text{w}}(V)}{D_{\text{core}}} \right]_{\text{MC}}$	1.0071	0.58 %	1.0080	0.60 %	1.0088	0.65 %
$S (\text{cm}^2)$	7.0700	0.04%	7.0700	0.04%	7.0700	0.04%
$N_{\text{DAPw}} (\text{Gy.cm}^2.\text{C}^{-1})$	$1.5856 \cdot 10^8$	0.83 %	$1.5511 \cdot 10^8$	0.68 %	$1.5525 \cdot 10^8$	0.89 %
$N_{\text{DAPw}}/N_{\text{DAPw}} (\varnothing=2 \text{ cm})$	1		0.973 (9)		0.974 (11)	

Table 6: Calibration factors of the large ionization chamber in terms of dose-area product for the three small fields studied at 6 MV.

Calibration factors in the 1 and 0.75 cm diameter beam are in good agreement within the uncertainties which suggests that a beam dimension exists under which the calibration factor of a large ionization chamber is independent of field size. The difference with the calibration factor in the 2 cm diameter field was first attributed to the small difference between the sensitive surface (3 cm diameter) and the field section: at 1.5 cm from the axis the absorbed dose is still around 5 % of the maximum dose in the 2 cm diameter beam, against less than 1 % for the two other field sizes (figure 7). Plotted on this figure is also the contribution of the simulated profile as a function of the axis distance. Data were normalized to the dose integral of the beam considered over a 3 cm diameter surface. The contribution of the profile at 1.5 cm from the axis is respectively 0.7 (5) %, 0.4 (1.9) % and 0.4 (2.7) % to the dose integral for the 2, 1 and 0.75 cm diameter beams.

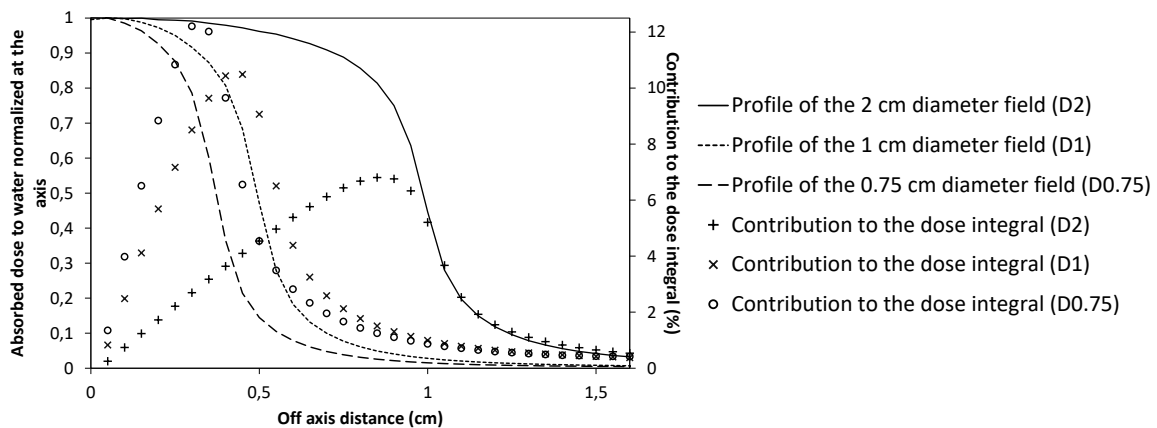


Figure 7: simulated dose profiles in a 2, 1 and 0.75 cm diameter field and the contribution of each corresponding ring to the integral of dose.

Thanks to simulated dose profiles one can determine the amount of energy that is deposited outside the 1.5 cm radius sensitive surface: as represented on figure 8, the contribution of the profile between 1.5 and 4 cm from the axis to the dose integral of a 4 cm radius surface is respectively of 13.3 %, 14.4 % and 17.7 % for the 2, 1 and 0.75 cm diameter beams. This contribution is due to the small out-of-field dose that is integrated over a large surface far from the axis and confirms that the dose-area product depends on the size of the dosimeters' surface. The variation of the cumulative contribution can be considered linear after 1.5 cm from the axis for all diameters showing that the sensitive surface of the dosimeters used can not explain a variation of the calibration factor with field size.

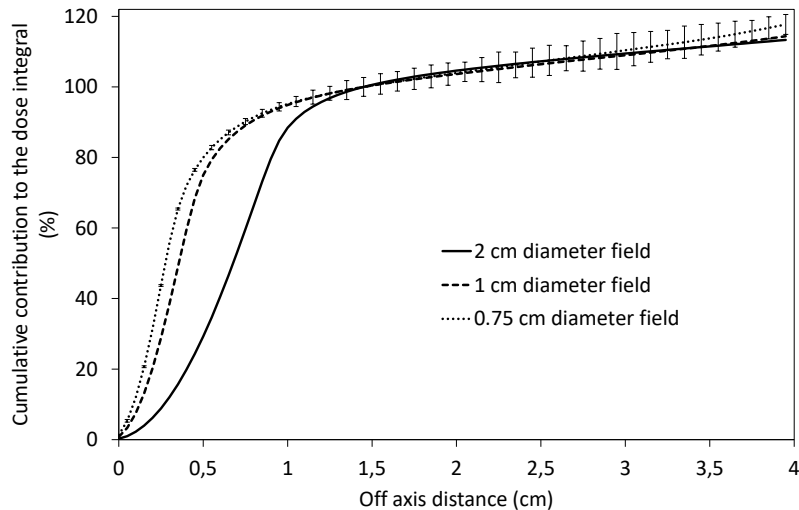


Figure 8: cumulative contribution to the dose integral as a function of offaxis distance for a 2, 1 and 0.75 cm diameter field. Data are normalised to the integral of dose over a 3 cm diameter surface (1.5 cm radius). For better clarity, only the uncertainties obtained for the 0.75 cm diameter field are plotted.

After further investigations, doubts were concentrated on a transfer measurement specific to the 2 cm diameter field to explain the difference in the calibration factors observed in table 6. However, no complementary data could be collected because the large ionization chamber was no longer operational. Measurements in a 1.5 cm diameter field would also have been necessary to confirm the trend observed for the two smallest field sizes. A new chamber prototype is under construction at the laboratory, with a sealing box made of crosslinked polystyrene in order to minimize the drift caused by the deformation in water.

5. Prospects

Although some improvements are still needed in primary laboratories for the determination of calibration factors in terms of dose-area product, this new approach raises the question of the transfer of such dosimetric references to users. Three options are available:

- A transfer in terms of dose-area product thanks to a commercially available large plane parallel ionization chamber like the PTW 34073 ($\varnothing=3.96$ cm) and PTW 34070 ($\varnothing=8.16$ cm). Since the diameter of their sensitive volume is different from the one of the large calorimeter built in this study, a correction factor would be needed to take into account the difference in the dose integrals measured by the chamber and the calorimeter. This correction factor would require the precise determination of out-of-field absorbed dose which is another challenging area.
- A transfer in terms of dose-area product thanks to a plane parallel ionization chamber with the same sensitive surface as the large calorimeter used for primary measurements. No correction factor would be needed which would lead to a smaller uncertainty on the calibration coefficient. However, this option would require either the commercialization of plane parallel chambers with a 3 cm sensitive surface or the construction of a new larger calorimeter. Since the sensitivity decreases when the sensitive surface increases, calorimetric measurements in small fields with

a sensitive surface larger than 3 cm seems difficult. If references were transferred in terms of dose-area product, the calibration certificate would have to include a precise 2D description of the beam for which the calibration coefficient was determined. Because the dose area product depends on the shape of the beam, medical physicists would also have to precisely measure the 2 D dose distribution of their beam at 10 cm depth.

- A transfer in terms of absorbed dose at a point, as currently recommended by the TRS398. A profile correction factor would be introduced to determine the absorbed dose delivered at a point from the measurement of a calorimeter which sensitive surface is larger than the beam section, similarly to (Sanchez-Doblado et al., 2007). Such factor can be expressed as:

$$k_{prof} = \frac{g(0) \int_0^R r dr}{\int_0^R g(r) r dr} \quad (1)$$

where $g(0)$ is the absorbed dose on the axis, $2\pi \int_0^R r dr$ is the sensitive surface of the calorimeter used for the primary measurement, $g(r)$ is the absorbed dose at a distance r from the axis and $2\pi \int_0^R g(r) r dr$ is the dose integral over the sensitive surface of the calorimeter. Primary laboratories would then be able to deliver calibration certificates in terms of absorbed dose to water at a point in small fields. Work is currently in progress at the laboratory to determine this profile correction factor using various detectors (EBT3, synthetic diamond and ion chamber).

6. Conclusion

Two large section detectors were specially designed and built: a graphite calorimeter and a plane parallel ionization chamber, both with a 3 cm diameter sensitive surface. Some difficulties were encountered during the sealing of the ionization chamber, causing the prototype to break at the end of the measurements. Calibration factors could be established in a 2, 1 and 0.75 cm diameter beam and were found independent of field size for the two smallest diameters. The comparison of simulations to measurements when the sensitive volume is fully and partially irradiated showed a disagreement.

Further investigations are still needed before considering the introduction of the dose-area product in radiotherapy departments. This study is nonetheless the first to realise absolute measurements in small fields. If the applicability of the dose-area product is verified and if a profile correction factor can be precisely defined, primary references could be determined and transferred to radiotherapy departments in terms of absorbed dose to water at a point in small fields. No correction factor $k_{Q_{msr},Q}^{f_{msr},f_{ref}}$ would then be required for output factors measurements.

ALFONSO, R., ANDREO, P., CAPOTE, R., HUQ, M. S., KILBY, W., KJALL, P., MACKIE, T. R., PALMANS, H., ROSSER, K., SEUNTJENS, J., ULLRICH, W. & VATNITSKY, S. 2008. A new formalism for reference dosimetry of small and nonstandard fields. *Medical Physics*, 35, 5179-5186.

- BENMAKHLOUF, H., SEMPAU, J. & ANDREO, P. 2014. Output correction factors for nine small field detectors in 6 MV radiation therapy photon beams: A PENELOPE Monte Carlo study. *Medical Physics*, 41, 041711.
- DAS, I. J., DING, G. X. & AHNESJO, A. 2008. Small fields: Nonequilibrium radiation dosimetry. *Medical Physics*, 35, 206-215.
- DAURES, J. & OSTROWSKY, A. 2005. New constant-temperature operating mode for graphite calorimeter at LNE-LNHB. *Physics in Medicine and Biology*, 50, 4035-4052.
- DAURES, J., OSTROWSKY, A. & RAPP, B. 2012. Small section graphite calorimeter (GR-10) at LNE-LNHB for measurements in small beams for IMRT. *Metrologia*, 49, S174-S178.
- DELAUNAY, F., KAPSCH, R.P., GOURIOU, J., ILLEMANN, J., KRAUSS, A., LE ROY, M., OSTROWSKY, A., SOMMIER, L. and VERMESSE, D. 2012 Comparison of absorbed-dose-to-water units for Co-60 and high-energy x-rays between PTB and LNE-LNHB. *Metrologia*, 49, S203-S206
- DJOUGUELA, A., HARDER, D., KOLLHOFF, R., RUHMANN, A., WILLBORN, K. C. & POPPE, B. 2006. The dose-area product, a new parameter for the dosimetry of narrow photon beams. *Zeitschrift Fur Medizinische Physik*, 16, 217-227.
- FAN, J., PASKALEV, K., WANG, L., JIN, L., LI, J., ELDEEB, A., MA, C. 2009. Determination of output factors for stereotactic radiosurgery beams. *Medical Physics*, 36, 5292-5300.
- IAEA-TRS398 2006. Absorbed Dose Determination in External Beam Radiotherapy: An International Code of Practice for Dosimetry based on Standards of Absorbed Dose to Water.
- ICRU 74, 2005. Patient dosimetry for X-rays used in medical imaging. *Journal of the International Commission on Radiation Units and measurements*, Vol 5, No 2
- IPEM 2010. Small field MV photon dosimetry. *Institute of physics and engineering in medicine*, Report 103.
- JCGM 2008. Evaluation of measurement data - Guide to the expression of uncertainty in measurement (GUM 1995 with minor corrections). *JCGM*, 100:2008
- KAWRAKOW I. 2000. Accurate condensed history Monte Carlo simulation of electron transport: I. EGSnrc, the new EGS4 version. *Medical Physics*, 27 485-98
- KAWRAKOW I., MAINEGRA-HING E., ROGERS D-W-O., TESSIER F., WALTERS B-R-B. 2009. The EGSnrc code System: Monte Carlo simulation of electron and photon transport. *NRCC Technical Report*, PIRS-701
- KRAUSS, A. and KAPSCH, R.P. 2014 Experimental determination of k_Q factors for cylindrical ionization chambers in 10 cm x 10 cm and 3 cm x 3 cm photon beams from 4 MV to 25 MV. *Physics in Medicine and biology*, 59, 4227-4246
- LE ROY, M. 2011. Etude de références dosimétriques nationales en radiothérapie externe - application aux irradiations conformationnelles. Thesis, *Sofia-Antipolis University of Nice*. https://hal.archives-ouvertes.fr/file/index/docid/725265/filename/memoire_M.LeRoy_VF.pdf
- LI, X., SOUBRA, M., SZANTO, M., GERIG, L. H. 1995. Lateral electron equilibrium and electron contamination in measurements of head-scatter using minihantoms and brass caps. *Medical physics*, 22, 1167.
- MOIGNIER, C., HUET, C. & MAKOVICKA, L. 2014. Determination of the $k_{Q_{clin}, Q_{msr}}^{f_{clin}, f_{msr}}$ correction factors for detectors used with an 800 MU/min CyberKnife® system equipped with fixed collimators and a study of detector response to small photon beams using a Monte Carlo method. *Medical physics*, 41, 071702.
- OSTROWSKY, A., BORDY, J.-M., DAURES, J., DE CARLAN, L., DELAUNAY, F. 2010. Dosimetry for small size beams such as IMRT and stereotactic radiotherapy. Is the concept of the dose at a point still relevant? Proposal for a new methodology, *CEA Report*, R-6243. Available at: http://www.nucleide.org/Publications/CEA-R-6243_PDS.pdf
- SANCHEZ-DOBLADO, F., HARTMANN, G. H., PENA, J., ROSELLO, J. V., RUSSIELLO, G. & GONZALEZ-CASTANO, D. M. 2007. A new method for output factor determination in MLC shaped narrow beams. *Physica Medica*, 23, 58-66.

Towards the use of a dose-area product for absolute measurements in small fields

SALVAT, F., FERNANDEZ-VAREA, J. M. & SEMPAN, J. PENELOPE-2006: A Code System for Monte Carlo Simulation of Electron and Photon Transport *In*: AGENCY, N. E., ed. Workshop Proceedings, 2006 Barcelona, Spain. Nuclear energy Agency.

UNDERWOOD, T.S.A., WINTER, H.C., HILL, M.A., FENWICK, J.D. 2013. Detector density and small field dosimetry: Integral versus point dose measurement schemes, *Medical Physics*, 40, 082102.